



Published in final edited form as:

Stem Cell Res. 2019 December ; 41: 101600. doi:10.1016/j.scr.2019.101600.

Robust generation of erythroid and multilineage hematopoietic progenitors from human iPSCs using a scalable monolayer culture system

Juan Pablo Ruiz^a, Guibin Chen^b, Juan Jesus Haro Mora^a, Keyvan Keyvanfar^c, Chengyu Liu^d, Jizhong Zou^e, Jeanette Beers^e, Hanan Bloomer^a, Husam Qanash^{a,f,g}, Naoya Uchida^a, John F. Tisdale^a, Manfred Boehm^b, Andre Larochelle^{a,*}

^aCellular and Molecular Therapeutics Branch, National Heart, Lung and Blood Institute (NHLBI), National Institutes of Health (NIH), 9000 Rockville, Bethesda, MD 20892, United States

^bTranslational Vascular Medicine Branch, NHLBI, NIH, Bethesda, MD 20892, United States

^cClinical Flow Core Facility, NHLBI, NIH, Bethesda, MD 20892, United States

^dTransgenic Core Facility, NHLBI, NIH, Bethesda, MD 20892, United States

^eiPSC Core Facility, NHLBI, NIH, Bethesda, MD 20892, United States

^fCollege of Applied Medical Sciences, University of Hail, Hail, Saudi Arabia

^gDepartment of Biology, The Catholic University of America, Washington, DC 20064, United States

Abstract

One of the most promising objectives of clinical hematology is to derive engraftable autologous hematopoietic stem cells (HSCs) from human induced pluripotent stem cells (iPSCs). Progress in translating iPSC technologies to the clinic relies on the availability of scalable differentiation methodologies. In this study, human iPSCs were differentiated for 21 days using STEMdiff™, a monolayer-based approach for hematopoietic differentiation of human iPSCs that requires no replating, co-culture or embryoid body formation. Both hematopoietic and non-hematopoietic cells were functionally characterized throughout differentiation. In the hematopoietic fraction, an early transient population of primitive CD235a⁺ erythroid progenitor cells first emerged, followed by hematopoietic progenitors with multilineage differentiation activity in vitro but no

This is an open access article under the CC BY-NC-ND license (<http://creativecommons.org/licenses/by-nc-nd/4.0/>).

*Corresponding author. larochea@nhlbi.nih.gov (A. Larochelle).

Author contributions

JPR and AL conceived and designed the study. GC, MB and AL were involved in the development of the monolayer iPSC differentiation platform, patent filing and licensing to STEMCELL Technologies, Inc. JPR performed the majority of experimental procedures with help from HQ, HB and AL. JJHM performed erythroid differentiation experiments and globin expression analysis with general overview and helpful suggestions from NU and JFT. KK sorted the various cell populations. JZ and JB reprogrammed human cells to MCND-TENS2 iPSC lines, and confirmed pluripotency by flow cytometry. CL performed the teratoma assays. JPR and AL wrote and edited the manuscript, with contributions from all other authors.

Declaration of Competing Interest

STEMdiff™ Hematopoietic Kit is registered under patent WO2015050963 A1. GC, MB and AL receive royalty income.

Supplementary materials

Supplementary material associated with this article can be found, in the online version, at doi:10.1016/j.scr.2019.101600.

long-term engraftment potential in vivo. In later stages of differentiation, a nearly exclusive production of definitive erythroid progenitors was observed. In the non-hematopoietic fraction, we identified a prevalent population of mesenchymal stromal cells and limited arterial vascular endothelium (VE), suggesting that the cellular constitution of the monolayer may be inadequate to support the generation of HSCs with durable repopulating potential. Quantitative modulation of WNT/ β -catenin and activin/nodal/TGF β signaling pathways with CHIR/SB molecules during differentiation enhanced formation of arterial VE, definitive multilineage and erythroid progenitors, but was insufficient to orchestrate the generation of engrafting HSCs. Overall, STEMdiff™ provides a clinically-relevant and readily adaptable platform for the generation of erythroid and multilineage hematopoietic progenitors from human pluripotent stem cells.

Keywords

Induced pluripotent stem cell; Hematopoietic stem and progenitor cell; STEMdiff™ hematopoietic differentiation kit; Monolayer differentiation system; Erythroid progenitor; Arterial vascular endothelium

1. Introduction

Long-term repopulating hematopoietic stem cells (HSCs) have durable self-renewal properties and multilineage potential, and can thus serve as lifelong reservoir for all blood cells (Doulatov et al., 2012). Hematopoietic stem and progenitor cell (HSPC) transplantation is the most established cellular replacement therapy for hematological and other conditions. However, the limited availability of HLA-matched donors and the associated severe acute and chronic complications significantly restrict allogeneic treatment options. In gene therapy applications, sufficient autologous HSPCs are not available for genetic modification in a wide variety of disorders, and methodologies for safe expansion of these rare cells are inexistent (Walasek et al., 2012). Induced pluripotent stem cell (iPSC)-based therapies are a promising alternative because of their potential to provide an unlimited source of autologous, patient-specific cells for transplantation. However, the stepwise addition of cytokines and morphogens used in most protocols to recapitulate the natural developmental process generally induces iPSCs to produce hematopoietic progenitors with limited engraftment and differentiation capability (Ditadi et al., 2017; Vo and Daley, 2015). The self-renewal and multilineage capacity of iPSC-derived hematopoietic cells can be enhanced by forced ectopic expression of hematopoietic transcription factors (TFs) (Doulatov et al., 2013; Sugimura et al., 2017). However, these protocols lack clinical relevance due to their low efficiency, poor scalability and the necessary use of integrating lentiviral vectors for constitutive expression of potentially oncogenic TFs.

In the developing mammalian embryo, blood is produced in consecutive waves (Ivanovs et al., 2017; Rytsov and Lagarkova, 2019; Yoder, 2014). The first wave of hematopoietic progenitors, dubbed “primitive”, occurs in the yolk sac blood islands (Frame et al., 2016). This primitive program is highly restricted, resulting primarily in the emergence of large, nucleated CD235a⁺ erythroid progenitor cells expressing embryonic globins, and in the production of some macrophage and megakaryocyte progenitors. A second wave of

hematopoietic potential, termed “definitive”, supplies lymphoid progenitor cells, as well as erythro–myeloid progenitors (EMPs) that produce red cells expressing predominantly adult-type γ - and β -globin molecules. The third wave is also considered “definitive” but is uniquely marked by the appearance of HSCs within the aorta-gonad-mesonephros (AGM) region of the developing embryo (de Bruijn et al., 2002, 2000). These cells are specified and bud off from hemogenic endothelium (HE), a distinct subset of vascular endothelium (VE) that directly changes fate into hematopoietic progenitors through a morphogenic process called endothelial-to-hematopoietic transition (EHT) (Boisset et al., 2010; Jaffredo et al., 1998; Zovein et al., 2008). Thus, HE with definitive hematopoietic potential must emerge for the ex vivo production of engraftable HSCs from human iPSCs.

Definitive multilineage HSPCs were shown to arise from HE lining arteries, but not veins, during development (Gordon-Keylock et al., 2013; Yzaguirre and Speck, 2016). This observation evokes the possibility that arterial specification of HE is necessary to initiate the definitive HPSC program and exploitation of this concept may facilitate the ex vivo production of engraftable HSCs (Slukvin and Uenishi, 2019; Uenishi et al., 2018). However, this hypothesis has been challenged and arterial specification of HE, while necessary, may not be sufficient for definitive HPSC formation (Slukvin and Uenishi, 2019). In addition, distinct cellular signaling pathways regulate the specification of primitive and definitive hematopoiesis in human iPSC cultures. Repression of nodal/activin signaling and activation of the WNT/ β -catenin pathway in mesodermal precursors are required to downregulate primitive and enrich for definitive hematopoietic programs (Kennedy et al., 2012; Ng et al., 2016; Sturgeon et al., 2014). Simultaneous modulation of these pathways at day 2 of culture has been shown to activate arterial genes and restore expression of several key hematopoietic regulators within the HOXA gene cluster that are commonly downregulated during human pluripotent stem cell differentiation (Ng et al., 2016; Park et al., 2018).

Most ex vivo methods for hematopoietic differentiation of iPSCs are based either on coculture with stromal cells or embryoid body (EB) formation (Kardel and Eaves, 2012). Recently, an alternative simple, monolayer-based, chemically-defined, and scalable differentiation protocol requiring no replating, coculture or EB formation has become available (STEMdiff™ Hematopoietic Kit, STEMCELL Technologies, Inc.). During differentiation, a supportive adherent monolayer rapidly forms, followed by the emergence of suspension hematopoietic cells that can be harvested at regular intervals during culture for analysis. This approach reproducibly yields enriched populations of CD43⁺CD45⁺CD34⁺ hematopoietic progenitors with functional activity in the colony-forming unit (CFU) assay. The simplicity and efficiency of the protocol have enabled secondary applications, such as differentiation of microglia (McQuade et al., 2018) and NK cells (Snyder et al., 2018), validation of CD34 fluorescent reporter human iPSC lines (Husa et al., 2018), mapping of human pluripotent stem cell differentiation pathways (Han et al., 2018), and investigation of a posttranscriptional regulatory circuitry for the maintenance and differentiation of pluripotent stem cells and HSPCs (Guzzi et al., 2018). In this study, we systematically examined the phenotype and function of hematopoietic and non-hematopoietic cells throughout differentiation, and provide evidence that this system can be adapted to move closer to a clinically-relevant protocol for the generation of definitive erythroid and multipotent hematopoietic progenitor cells.

2. Methods

2.1. Generation and culture of iPSCs

Peripheral blood CD34⁺CD38⁻ cells mobilized from healthy donors were reprogrammed into iPSCs (MCND-TENS2, registered at <https://hpscereg.eu/cell-line/RTIBDi001-A>) using the integration-free CytoTune2.0 Sendai virus reprogramming kit (A16517, Thermo Fisher Scientific) following the method previously reported (Beers et al., 2015; Chen et al., 2011). Pluripotency was confirmed by teratoma formation assay, G-banding karyotype and flow cytometry for TRA-1-60 and NANOG markers as previously described (Baskfield et al., 2019). iPSCs were maintained on 6-well tissue culture plates thinly coated with Matrigel® (Corning, 354230) in Essential 8™ (E8) Medium (A1517001, Thermo-Fisher). Culture medium was changed daily and iPSCs were split every three to four days. Briefly, medium was aspirated and wells were sequentially washed with phosphate buffered saline (PBS) or 0.5 mM EDTA in PBS (PBS/EDTA). Cells were then dissociated in PBS/EDTA 0.5 mM for 2–3 min. PBS/EDTA was aspirated and replaced with 1 mL E8 medium containing 1.25 μM ROCK inhibitor (Y0503, Sigma). Cells were pipetted 3–4 times using a P1000 pipette to dissociate into small to medium sized clusters, and split onto new 6-well plates at various dilutions.

2.2. Hematopoietic differentiation of human iPSCs

MCND-TENS2 iPSCs were differentiated for 21 days using the STEMdiff™ Hematopoietic Kit (05310, STEMCELL Technologies, Inc.). Reproducibility of this approach to efficiently generate multilineage HSPCs was confirmed with additional iPSC lines (Table S1), but the extensive characterization of the cellular constituents that form throughout differentiation, as reported in this study, was performed with MCND-TENS2 only. Briefly, one day (D) before differentiation (D-1), iPSCs were split as described above, and cluster concentrations were calculated. A total of 20–35 clusters were transferred per well into a Matrigel-coated 12-well plate and cultured overnight. On D0 of differentiation, medium A (containing bFGF, BMP4, VEGFA) was added to promote mesodermal differentiation and a half medium A change was done on D2. In select experiments, WNT/β-catenin agonist CHIR99021 (SML1046, Sigma) and activin/nodal/TGFβ antagonist SB431542 (S4317, Sigma) were added on D2 at a final concentration of 3 μM for 24–36 h. On D3 of differentiation, supernatant was removed and hematopoietic differentiation medium B (containing bFGF, BMP4, VEGFA, SCF, Flt3L, TPO) was added, followed by half-medium change on day 5, 7, 10, 12, 14, 17, and 19. On days when medium was changed, supernatant and monolayer cells were harvested for analysis. To completely detach the monolayer and clusters of cells from the plastic surface, Accutase™ (07920, STEMCELL Technologies, Inc.) was added to each well for 10 min at 37 °C and cells were vigorously pipetted up and down to ensure complete recovery. Cells were then filtered through a 40 μM cell strainer, counted, and prepared for further analysis.

2.3. Flow cytometry and fluorescence-activated cell sorting (FACS)

Cells were stained with antibodies (Table S2), following manufacturer's instructions and analyzed on an LSRII Fortessa analyzer (Becton Dickinson). Complete gating strategies used for all flow cytometry analyses in this study are shown in Fig. S1 (A to F). For

gene expression, CFU assays, MSC differentiation, and mouse transplantation studies, cell populations were sorted on a FACS Aria (Becton Dickinson) with a 100 μ m nozzle.

2.4. Gene expression by real-time qPCR

RNA was extracted and purified using directions of the RNeasy Micro Kit (74004, Qiagen). To assess HOXA gene expression, real-time qPCR was done using TaqMan RNA-to-Ct 1-Step Kit (4392653, Applied Biosystems) on a BioRad C1000 touch system and all samples were multiplexed to include an internal *GAPDH* control. Primers and probes used for real-time qPCR are listed in Table S3. Error bars were calculated using SEM for C_T values to calculate the upper and lower boundaries of the 95% confidence interval, which were then log transformed in the same way as the mean (2^{-C_T}). Two-way unpaired Student's t-tests were done on untransformed C_T values.

2.5. CFU assays

Human CFU assays were performed as per manufacturer's instructions (04445, STEMCELL Technologies, Inc.). Briefly, 9000 and 4500 total supernatant cells for control and CHIR/SB samples, respectively, were suspended in 300 μ L of DMEM/2% FBS, which was then added to the methocult tube and vortexed. Following 5 min to allow for bubble dissipation, 1.1 mL of the medium was plated onto 35 \times 10 mm style tissue-culture dishes (353001, Corning) for 1500 to 3000 cells per plate. Colonies were scored 17– 20, and 14 days following plating for control and CHIR/SB samples, respectively.

2.6. NSG mouse transplantation

6- to 12-week-old female NSG mice (Jackson Laboratory, stock #05557) were sublethally irradiated (270 cGy) 24 h before tail-vein injection of 3×10^4 to 3×10^5 CD43⁺CD45^{+/-} supernatant cells harvested and sorted at day 10 and 12 of iPSC differentiation. Bone marrow (BM) was collected 16 weeks post-transplantation and stained with human CD45-PE (clone HI30, BD Pharmingen). Animals were housed and handled in accordance with the guidelines set by the Committee on Care and Use of Laboratory Animals of the Institute of Laboratory Animal Resources, National Research Council (DHHS publication No. NIH 85–23), and the protocol was approved by the Animal Care and Use Committee of the NHLBI.

2.7. Mesenchymal stromal cell (MSC) differentiation

To confirm MSC identify, CD43⁻CD45⁻ monolayer cells were sorted at various days of culture and differentiated per manufacturer's instructions into adipocytes (A1007001, Thermo Fisher Scientific), chondrocytes (A1007101, Thermo Fisher Scientific), and osteocytes (A1007201, Thermo Fisher Scientific). For comparison, control MSCs derived from the BM of a healthy individual were differentiated following the same procedures.

2.8. Erythroid differentiation

For determination of globin chain composition, supernatant and monolayer cells were collected at day 7 and 17 of culture, and differentiated toward the erythroid lineage as previously described (Fujita et al., 2016; Uchida et al., 2017). Briefly, cells were cultured

on irradiated OP9 cells (American Type Culture Collection (ATCC)) in Medium B with the addition of 5 U/mL erythropoietin (EPO; Amgen) and 5 ng/mL interleukin-3 (IL3; R&D Systems). Two days later, the floating cells were transferred into freshly irradiated OP9 feeder plates using an erythroid expansion media based on Iscove's Modified Dulbecco's Medium (IMDM; Sigma Aldrich) supplemented with 10 ng/mL stem cell factor (SCF; R&D Systems), 1 ng/mL IL3, 2 U/mL EPO, 1 μ M estradiol (Pfizer), 1 μ M dexamethasone (VETone, Boise), and 20% Knockout Serum Replacement (KSR, Thermo Fisher Scientific). Five days later, the medium was changed to a maturation erythroid medium containing IMDM, 2% bovine serum albumin (BSA; Roche), 0.56 mg/mL transferrin (Sigma Aldrich), 2 mM L-glutamine (Thermo Fisher Scientific), 2 U/mL EPO, 10 ng/mL insulin (Lilly), and 20% KSR, and the cells were cultured for another 8 to 10 days.

2.9. Reverse phase-high performance liquid chromatography (RP-HPLC)

The globin protein content of differentiated erythroid cells was evaluated by RP-HPLC as previously described (Uchida et al., 2018, 2017). Briefly, erythroid cells were harvested and washed 3 times with PBS followed by a lysis step using HPLC grade water. The lysates were mixed with 10% of 100 mM Tris (2-carboxyethyl) phosphine (TCEP, Thermo Fisher Scientific) and incubated for 5 min. Then, the lysates plus TCEP were mixed 1:1 with a solution containing 0.1% trifluoroacetic acid (TFA) and 32% acetonitrile (Honeywell Burdick & Jackson). The mixtures were centrifuged at 16000 g for 5 min and the supernatant was injected in an Agilent 1100 HPLC (Agilent Technologies) equipped with a reverse phase column, Aeris 3.6 μ m Widepore C4 200 \AA (25034.6 mm, Phenomenex) with two solvents: solvent A, 0.12% TFA in water and solvent B, 0.08% TFA in acetonitrile using a flow of 0.7 mL per minute for 50 min.

2.10. Statistical analysis

Results were analyzed with GraphPad Prism Software, using unpaired Student t-tests. Results are displayed as mean \pm SEM and * signifies $p < 0.05$, ** $p < 0.01$, *** $p < 0.001$, and **** $p < 0.0001$.

3. Results

3.1. Robust production of an adherent monolayer and supernatant hematopoietic cells during differentiation of human iPSCs

Human iPSCs reprogrammed from CD34⁺CD38⁻ cells of a healthy volunteer (MCND-TENS2, Fig. S2, A to C) were subjected to hematopoietic differentiation for 21 days using the STEMdiff™ monolayer approach. In select experiments, we also explored the effects of adding the WNT/ β -catenin agonist CHIR99021 (CHIR) and the activin/nodal/TGF β antagonist SB431542 (SB), from differentiation day 2 to 3 (Fig. 1A). Under culture conditions that favored mesodermal specification (medium A, day 0 to 3), an adherent monolayer rapidly formed. With the subsequent addition of hematopoietic cytokines (medium B, day 3 to 21), hematopoietic clusters emerged from the monolayer before their eventual release in the supernatant fraction (Fig. 1B).

To systematically characterize cells arising from this system, supernatant and monolayer populations were harvested together at regular intervals between day 5 and 21 of differentiation (Fig. 1A). Hematopoietic cells were characterized by varying expression of CD43, the earliest marker of human hematopoietic commitment, and by gradual acquisition of the pan-hematopoietic marker CD45 (CD43⁺CD45^{+/-}). In contrast, non-hematopoietic cells formed a distinct population expressing neither markers (CD43⁻CD45⁻) (Fig. 1C).

In the first phase of differentiation (day 5 to 9), the non-hematopoietic population comprised most cells in culture with a modest relative contribution from the hematopoietic fraction (Fig. 1D, E). Between day 10 and 14, we observed an increase in percentages (Fig. 1D) and absolute numbers (Fig. 1E) of hematopoietic cells, and a concomitant decrease in the proportion of non-hematopoietic cells likely resulting from an EHT process in culture. Hematopoietic cells were detected at a peak frequency of $69.1 \pm 4.3\%$ with an average yield of $1.1 \pm 0.1 \times 10^6$ cells per 20–35 iPSC clusters (one well of a 12-well plate) at day 12 of culture. In the third stage of culture (day 15 to 21), both hematopoietic and non-hematopoietic fractions contributed equally (Fig. 1D), but at a reduced total output (Fig. 1E) in part due to decreased cell viability (Fig. S3). These data collectively show robust differentiation of human iPSCs into a supportive adherent monolayer from which hematopoietic clusters and suspension cells develop for up to 21 days in culture.

3.2. Successive emergence of hematopoietic populations during differentiation of human iPSCs

To determine whether hematopoietic differentiation of human iPSCs using the STEMdiff™ monolayer system can provide a suitable ex vivo model to study the emergence of hematopoiesis, we characterized the hematopoietic CD43⁺CD45^{+/-} fraction throughout differentiation by flow cytometry and functional assays.

We observed the formation of 3 successive populations of cells, as defined by expression of the CD34 hematopoietic progenitor cell marker. The first hematopoietic cells to arise were predominantly CD34⁻CD45⁻ with a distinct CD235a⁺ erythroid progenitor phenotype. These cells peaked at day 7 and rapidly disappeared, evoking the transient nature of primitive erythroid progenitor cells that form during wave one of hematopoiesis in the developing embryo (Fig. 2A, B). The second population of hematopoietic cells was enriched in CD34^{hi}CD45^{lo} multipotent HSPCs. The maximum production of these cells was observed at day 12 of differentiation, comprising $17.8 \pm 0.6\%$ of the hematopoietic cells and producing $1.7 \pm 0.2 \times 10^5$ HSPCs per well (Fig. 2A, B). In the third phase of hematopoietic production, HSPCs gradually lost CD34 and upregulated expression of surface CD45, consistent with their progressive differentiation in extended cultures. By day 17 of culture, CD34^{lo/-}CD45⁺ cells accounted for $81.9 \pm 1.9\%$ of the hematopoietic fraction, with an average yield of $3.7 \pm 0.2 \times 10^5$ cells per well, and this contribution persisted through day 21 (Fig. 2A,B).

We next sorted CD43⁺CD45^{+/-} hematopoietic cells to assess their multilineage differentiation potential in clonogenic progenitor assays. Colony-forming progenitors were detected throughout differentiation at frequencies ranging from 12.5 ± 4.8 to 30.3 ± 2.2 progenitors per 10^3 hematopoietic cells (Fig. 2C). At culture days when CD34^{hi}CD45^{lo}

HSPCs were found to be most abundant by flow cytometry (day 10 to 14), growth of both myeloid (CFU-G, CFU-M and CFU-GM) and erythroid (BFU-E and CFU-E) colonies was observed. A progressive rise in BFU-E/CFU-E colonies was subsequently detected during culture, with a nearly exclusive erythroid contribution by day 21 (Fig. 2C). To evaluate the developmental stage of erythroid progenitors, we quantified globin chains by RP-HPLC in RBCs differentiated from day 7 and day 17 hematopoietic cells (Fig. 2D). At day 7, embryonic (ϵ) globins prevailed, comprising $68.4 \pm 2.6\%$ of total β -globin series expression. In contrast, red cells derived from day 17 suspension cells predominantly expressed adult-type γ - and β -globins, whereas ϵ -globins contributed much less compared with day 7 ($11.1 \pm 2.1\%$ of β -globin series expression). These results were consistent with primitive (first wave) and definitive (second wave) hematopoiesis at day 7 and 17 of culture, respectively.

To determine whether the $CD43^+CD45^+$ hematopoietic fractions at different stages of differentiation might contain hematopoietic cells with long-term repopulating potential, we first searched for cells with a $CD34^+CD38^-CD45RA^-CD90^+CD49f^+$ phenotype which enables the highest reported purity of human HSCs (Notta et al., 2011). Immunophenotypic HSCs (Fig. S4A) were detected in the hematopoietic fraction primarily between day 10 and 14, with a maximum yield of $1.4 \pm 0.5 \times 10^4$ cells per well at day 12 of differentiation (Fig. 2E). However, these cells did not result in efficient, long-term engraftment after transplantation in immuno-deficient (NSG) mice, consistent with the previously reported dissociation between stem cell repopulating function and cell surface phenotype in cultured cells (Fig. S4B, left panel) (Dorrell et al., 2000).

From these data, we infer that hematopoietic differentiation of human iPSCs with STEMdiff™ enables the sequential development of hematopoietic cells with features of primitive wave one-hematopoiesis (peak at day 7), definitive multilineage HSPCs with potent colony formation activity in vitro but limited engraftment potential in vivo (peak at day 12), and definitive erythroid-committed progenitors expressing adult-type globin chains (peak at day 17 to 21).

3.3. Abundant mesenchymal cells and limited arterial endothelium formation during human iPSC differentiation

To identify possible causes for the lack of durable repopulating potential of iPSC-derived HSPCs in this system, we sought to identify the cellular constituents of the $CD43^-CD45^-$ non-hematopoietic fraction that supports hematopoiesis during differentiation. Because definitive HSPCs emerge from HE in close association with the VE (de Bruijn et al., 2002; Frame et al., 2016), we first queried whether non-hematopoietic cells expressed VE-defining markers, including VE-cadherin (CD144) and high levels of surface CD34 ($CD144^+CD34^{hi}$). Non-hematopoietic cells expressing neither marker ($CD144^-CD34^-$) were recently shown to characterize a population of mesenchymal cells (Guibentif et al., 2017). We found that most non-hematopoietic cells throughout differentiation lacked CD144 and CD34 expression, representing up to $92.5 \pm 2.5\%$ of this population at day 21. In contrast, $CD144^+CD34^{hi}$ VE accounted for only a limited proportion of the non-hematopoietic fraction, with a maximal contribution of $7.8 \pm 2.0\%$ at day 5 that steadily declined during culture (Fig. 3A, B). The emergence of HE, a distinct $CD73^-$ endothelial

lineage within the VE population (Choi et al., 2012; Ditadi et al., 2015), was observed at day 5 of culture, representing a substantial proportion of CD144⁺CD34^{hi} VE (55.7 ± 1.8%) but only 5.5 ± 1.8% of the total non-hematopoietic fraction. No significant population of HE was detected after day 5 of differentiation (Fig. 3A, B).

To further characterize the CD144⁻CD34⁻ fraction, we assayed for expression of the surface markers CD90, CD73, and CD105, commonly used to identify mesenchymal stromal cells (MSCs), a major component of the adult BM niche. We observed a progressive increase in the percentage of cells with an MSC phenotype during differentiation (Fig. 3C,D), contributing up to 61.5 ± 3.9% of the non-hematopoietic cells at day 21. Because MSCs characteristically differentiate to adipocytes, chondrocytes and osteocytes in vitro, we tested the trilineage differentiation potential of day 21 non-hematopoietic cells. In agreement with the observed MSC phenotype, we detected adipocytes, chondrocytes and osteocytes, although differentiation to adipocytes was more limited compared to control MSCs derived from primary BM specimens (Fig. 3E).

Because HE and HSPCs are associated with arteries, not veins, in the developing embryo (Gori et al., 2015; Hadland et al., 2015; Uenishi et al., 2018), we next investigated whether arterial endothelium could be identified within the CD144⁺CD34^{hi} VE population. Based on distinct expression of the surface markers CD184 and CD73, arterial and venous VE progenitors were previously reported to segregate to the CD73^{mid}CD184⁺ and CD73^{hi}CD184⁻ fractions, respectively (Ditadi et al., 2015). We observed that CD73^{hi}CD184⁻ venous VE accounted for most of the CD144⁺CD34^{hi} endothelial fraction throughout differentiation. In contrast, low percentages of CD73^{mid}CD184⁺ arterial VE were detected only in the first phase of differentiation, with a maximal contribution of 3.6 ± 1.4% of the non-hematopoietic population at day 7 of culture. These cells subsequently declined and became undetectable after day 12 of differentiation (Fig. 3F, G). Similarly, arterial-type HE (DLL4⁺CD184^{+/-} HE), previously proposed as an essential prerequisite for establishing definitive lympho-myeloid program (Ditadi et al., 2015; Uenishi et al., 2018), was not detected during culture (Fig. 3G and Fig. S5). Thus, the limited arterial endothelium and distinct abundance of mesenchymal cells within the supportive non-hematopoietic fraction provide a sensible explanation for the lack of engraftment potential of iPSC-derived HSPCs produced with this approach.

3.4. CHIR/SB molecules increase arterial endothelium formation during the early phase of human iPSC differentiation

Because simultaneous modulation of nodal/activin and WNT/ β -catenin pathways in mesodermal precursors was previously shown to activate arterial genes, restore expression of the hematopoietic HOXA gene cluster and promote definitive hematopoiesis (Ng et al., 2016; Park et al., 2018), we examined the effect of supplementing the culture medium with the WNT/ β -catenin agonist CHIR99021 (CHIR) and nodal/activin inhibitor SB431542 (SB) at day 2 of STEMdiffTM iPSC differentiation for a period of 24–36 h (Fig. 1A).

Addition of CHIR/SB led to a global increase in the percentages (Fig. 4A) and numbers (Fig. S6A) of CD43⁻CD45⁻ non-hematopoietic cells on most days of differentiation compared to control cultures. In the early phase of differentiation, this increase stemmed

primarily from a rise in VE formation (Fig. 4B), and percentages of arterial (Fig. 4C) but not venous (Fig. 4D) VE increased in the presence of CHIR/SB. In addition, HOXA5, HOXA9 and HOXA10 transcription factors, previously shown to facilitate engraftment of iPSC-derived HSPCs (Sugimura et al., 2017), were 2 to 4-fold more expressed in day 7 VE derived from CHIR/SB cultures compared to controls. However, the CHIR/SB-mediated effect on the production of VE was not sustained after day 7 of culture (Fig. 4B), and CD144⁻CD34⁻ mesenchymal cells continued to account for up to 95% of the non-hematopoietic fraction in the late phase of differentiation (Fig. 4F).

3.5. CHIR/SB molecules suppress primitive hematopoiesis and promote definitive HSPC formation during human iPSC differentiation

We next investigated whether the early increase in VE formation observed in the presence of CHIR/SB influenced hematopoietic development. Addition of CHIR/SB led to an overall decrease in the percentages (Fig. 5A) and numbers (Fig. S6B) of hematopoietic cells relative to control cultures. As reported in other systems (Sturgeon et al., 2014), we observed CHIR/SB-mediated suppression of the primitive wave of CD34⁻CD45⁻CD235a⁺ erythroid progenitor cells (Fig. 5B), and a rise in percentages of CD34^{hi}CD45^{lo} definitive HSPCs (Fig. 5C) with a concomitant reduction in percentages of CD34^{lo/-}CD45⁺ cells in late stages of differentiation compared to controls (Fig. 5D). In colony forming assays, the frequency of progenitors with multilineage differentiation capacity was similar between sorted CHIR/SB and control hematopoietic cells at day 10 to 14 of culture (Fig. 5E). In contrast, the progressive rise in BFU-E/CFU-E frequency previously observed from day 17 to 21 of the standard differentiation protocol was further enhanced by addition of CHIR/SB (Fig. 5E). In RBCs differentiated from day 17 supernatant cells of CHIR/SB cultures, ϵ -globin expression was further decreased ($5.8 \pm 1.1\%$ of total β -globin series expression) compared to controls ($11.1 \pm 2.1\%$), and a congruent increase in adult-type γ - and β -globins was observed (Fig. 5F).

Next, we assessed whether CHIR/SB enabled the emergence of the third wave of definitive HSPCs with engraftment potential during iPSC differentiation. Immunophenotypic HSCs were readily detected at day 10 to 14 of differentiation at levels similar to control cultures (Fig. 5G). Addition of CHIR/SB also increased HOXA5, HOXA9 and HOXA10 expression 3 to 6-fold in supernatant cells harvested at day 12 compared to controls (Fig. 5H). However, these cells did not sustain long-term hematopoietic engraftment in NSG mouse recipients (Fig. S4B, right panel). Together, these results indicate that addition of CHIR/SB during mesodermal specification suppresses primitive hematopoiesis, promotes the second wave of definitive hematopoiesis, but is insufficient to enable generation of functional HSCs.

4. Discussion

Spontaneous production of cells with properties of normal transplantable HSCs, independent of ectopic expression of potentially oncogenic transcription factors, has to date eluded the field. In this study, we systematically characterized an alternative monolayer-based culture system that may facilitate investigation of novel strategies for the differentiation of human iPSCs into fully functional HSCs. The utility of this approach hinges on its scalability for

clinical and research applications, and its simple, adaptable experimental design requiring no replating, EB formation or coculture on stromal elements.

In the hematopoietic fraction, we observed transient production of primitive CD235a⁺ erythroid progenitors followed by robust generation of HSPCs with clonogenic progenitor activity in vitro, a bona fide HSC immunophenotype (CD34⁺CD38⁻CD90⁺CD45RA⁻CD49f⁺), but no long-term engraftment potential in vivo. Thus, similar to other iPSC hematopoietic differentiation protocols, STEMdiff™ primarily recapitulates the first (primitive) and second (definitive) developmental wave of hematopoiesis observed in the yolk sac of developing embryos.

To understand the possible causes underpinning the absence of engraftable HSCs in this system, we examined the cellular constituents of the supportive non-hematopoietic niche. We first identified a prevalent population of immunophenotypic mesenchymal cells throughout differentiation. Perivascular mesenchymal cells are known to interact with HSPCs and maintain their activity in the adult BM niche (He et al., 2017). However, their role in promoting HSPC development during ontogeny has not been demonstrated. Instead, mesenchymal cells have been implicated as components of the niche in the yolk sac controlling primitive erythroid cell maturation (Sturgeon et al., 2012). Further investigation is needed to fully understand whether these cells may offer inhibitory signals that preclude normal developmental switch to third wave definitive hematopoiesis during iPSC differentiation. We also found limited VE production and arterial specification within the non-hematopoietic fraction that may account for the lack of engrafting HSCs in culture. Indeed, recent advances propose that formation of these cells is restricted to arterial vessels during ontogeny (Gordon-Keylock et al., 2013; Yzaguirre and Speck, 2016). The arterial-specification model is supported in part by the demonstration of shared signaling requirements for both arterial identity acquisition and HSPC development (Burns et al., 2009; Gering and Patient, 2005; Kumano et al., 2003; Lawson et al., 2001, 2002; Robert-Moreno et al., 2005, 2008), and by the observation of selective impairment of hematopoiesis in the arteries of mice with knock-out of the artery-specific gene Ephrin B2 (Adams et al., 1999; Chen et al., 2016). Thus, in keeping with this model, arterial VE and HE are likely inadequate to support the generation of bona fide engrafting HSCs in culture. Ongoing single cell RNA sequencing (RNA-seq) and ATAC-seq studies will elucidate differences in gene expression and chromatin accessibility between bona fide and iPSC-derived HSPCs, and inform possible strategies to overcome the engraftment deficit.

Our study provides proof-of-principle that the monolayer iPSC differentiation system is readily amenable to simple, clinically applicable modifications to improve hematopoietic output. Quantitative modulation of WNT/β-catenin and activin/nodal/TGFβ signaling pathways by one-time addition of CHIR/SB molecules during mesodermal specification enhanced arterial VE and increased HOXA gene expression and definitive HSPC formation. However, consistent with previous studies (Kennedy et al., 2012; Ng et al., 2016; Sturgeon et al., 2014), this approach alone was insufficient to orchestrate the formation of functional HSCs and additional revisions to this system will be required. Addition of retinoid acid, a morphogen with a documented role in de-repressing HOXA genes (Deschamps and van Nes, 2005; Dou et al., 2016; Mazzoni et al., 2013; Montavon and Soshnikova, 2014)

and in embryonic HSPC development (Chanda et al., 2013; Goldie et al., 2008), may be required to complete the mesodermal patterning initiated by CHIR/SB. A recent study also revealed that overexpression ETS1, an EST family transcription factor involved in arterial fate control, or direct manipulation of MAPK/ERK signaling at the mesodermal stage led to an increase in arterial VE and definitive HSPCs (Park et al., 2018). It will be of interest to determine whether a combined approach to modulate MAPK/ERK, WNT/ β -catenin and activin/nodal/TGF β signaling pathways at this stage of differentiation can provide a synergy sufficient to further promote definitive hematopoiesis and the generation of engrafting HSCs.

In addition to the sequential emergence of developmental hematopoietic waves recognized in this study, our data also uncovered a nearly exclusive shift to definitive erythroid growth in later stages of differentiation that could be further enhanced by simple addition of CHIR/SB during mesodermal specification. Notably, this late erythropoietic up-surge occurred concomitantly with a rise in MSCs within the non-hematopoietic fraction. This observation coheres with the previously described erythroid commitment of human HSPCs co-cultured in the presence of MSCs (Alakel et al., 2009; Perucca et al., 2017). In one study (Perucca et al., 2017), a significant enrichment of genes implicated in heme metabolism and a parallel downregulation of pathways involved in lymphoid and myeloid differentiation were noted in co-cultured CD34⁺ HSPCs. However, the precise molecular mechanism by which MSCs promote erythroid differentiation remains uncertain. The monolayer hematopoietic differentiation approach used in this study could provide a useful platform to identify prospective MSC-derived soluble factors implicated in erythroid maturation. Importantly, the STEMdiff™ system could be exploited to facilitate erythroid differentiation of iPSCs established from patients with hemoglobinopathies or various congenital BM failures and anemias affecting early erythropoiesis. The robust generation of patient-specific erythroid progenitors could have considerable implications, including *ex vivo* modeling of disease pathophysiology, preclinical screening of gene therapy strategies, and specific testing of novel therapeutics against disease-relevant human cells.

Supplementary Material

Refer to Web version on PubMed Central for supplementary material.

Acknowledgments

The authors thank J. Philip McCoy, Ph.D. and the NHLBI Flow Cytometry Core staff for sorting iPSC-derived cells; David Stroncek, M.D. and the NIH Department of Transfusion Medicine (DTM) and Cell Processing Section (CPS) staff for apheresis, selection and cryopreservation of human CD34⁺ cells; Tatyana Worthy, R.N., and the out-patient clinic nursing staff for recruiting normal volunteers and providing G-CSF administration teaching to healthy subjects; the mouse core facility staff for excellent animal care; Zu-xi Yu, M.D. Ph.D. of the pathology core of the NHLBI, NIH for sectioning and staining the teratomas. This work was supported by the intramural research program of the NHLBI, NIH (grant Z99 HL999999), and the Howard Hughes Medical Institute, HHMI (JPR, doctoral Gilliam Fellowship).

References

Adams RH, Wilkinson GA, Weiss C, Diella F, Gale NW, Deutsch U, Risau W, Klein R, 1999. Roles of ephrinB ligands and EphB receptors in cardiovascular development: demarcation of arterial/venous

- domains, vascular morphogenesis, and sprouting angiogenesis. *Genes Dev.* 13, 295–306. [PubMed: 9990854]
- Alakel N, Jing D, Muller K, Bornhauser M, Ehninger G, Ordemann R, 2009. Direct contact with mesenchymal stromal cells affects migratory behavior and gene expression profile of CD133+ hematopoietic stem cells during ex vivo expansion. *Exp. Hematol* 37, 504–513. [PubMed: 19216019]
- Baskfield A, Li R, Beers J, Zou J, Liu C, Zheng W, 2019. An induced pluripotent stem cell line (TRNDi009-C) from a Niemann-Pick disease type A patient carrying a heterozygous p.L302P (c.905T > C) mutation in the SMPD1 gene. *Stem Cell Res.* 38, 101461. [PubMed: 31132580]
- Beers J, Linask KL, Chen JA, Siniscalchi LI, Lin Y, Zheng W, Rao M, Chen G, 2015. A cost-effective and efficient reprogramming platform for large-scale production of integration-free human induced pluripotent stem cells in chemically defined culture. *Sci. Rep* 5, 11319. [PubMed: 26066579]
- Boisset JC, van Cappellen W, Andrieu-Soler C, Galjart N, Dzierzak E, Robin C, 2010. In vivo imaging of haematopoietic cells emerging from the mouse aortic endothelium. *Nature* 464, 116–120. [PubMed: 20154729]
- Burns CE, Galloway JL, Smith AC, Keefe MD, Cashman TJ, Paik EJ, Mayhall EA, Amsterdam AH, Zon LI, 2009. A genetic screen in zebrafish defines a hierarchical network of pathways required for hematopoietic stem cell emergence. *Blood* 113, 5776–5782. [PubMed: 19332767]
- Chanda B, Ditadi A, Iscove NN, Keller G, 2013. Retinoic acid signaling is essential for embryonic hematopoietic stem cell development. *Cell* 155, 215–227. [PubMed: 24074870]
- Chen II, Caprioli A, Ohnuki H, Kwak H, Porcher C, Tosato G, 2016. EphrinB2 regulates the emergence of a hemogenic endothelium from the aorta. *Sci. Rep* 6, 27195. [PubMed: 27250641]
- Chen G, Gulbranson DR, Hou Z, Bolin JM, Ruotti V, Probasco MD, Smuga-Otto K, Howden SE, Diol NR, Propson NE, Wagner R, Lee GO, Antosiewicz-Bourget J, Teng JM, Thomson JA, 2011. Chemically defined conditions for human iPSC derivation and culture. *Nat. Methods* 8, 424–429. [PubMed: 21478862]
- Choi KD, Vodyanik MA, Togarrati PP, Suknuntha K, Kumar A, Samarjeet F, Probasco MD, Tian S, Stewart R, Thomson JA, Slukvin II, 2012. Identification of the hemogenic endothelial progenitor and its direct precursor in human pluripotent stem cell differentiation cultures. *Cell Rep.* 2, 553–567. [PubMed: 22981233]
- de Bruijn MF, Ma X, Robin C, Ottersbach K, Sanchez MJ, Dzierzak E, 2002. Hematopoietic stem cells localize to the endothelial cell layer in the midgestation mouse aorta. *Immunity* 16, 673–683. [PubMed: 12049719]
- de Bruijn MF, Speck NA, Peeters MC, Dzierzak E, 2000. Definitive hematopoietic stem cells first develop within the major arterial regions of the mouse embryo. *EMBOJ.* 19, 2465–2474.
- Deschamps J, van Nes J, 2005. Developmental regulation of the Hox genes during axial morphogenesis in the mouse. *Development* 132, 2931–2942. [PubMed: 15944185]
- Ditadi A, Sturgeon CM, Keller G, 2017. A view of human haematopoietic development from the Petri dish. *Nat. Rev. Mol. Cell. Biol* 18, 56–67. [PubMed: 27876786]
- Ditadi A, Sturgeon CM, Tober J, Awong G, Kennedy M, Yzaguirre AD, Azzola L, Ng ES, Stanley EG, French DL, Cheng X, Gadue P, Speck NA, Elefanty AG, Keller G, 2015. Human definitive haemogenic endothelium and arterial vascular endothelium represent distinct lineages. *Nat. Cell. Biol* 17, 580–591. [PubMed: 25915127]
- Dorrell C, Gan OI, Pereira DS, Hawley RG, Dick JE, 2000. Expansion of human cord blood CD34(+)CD38(–) cells in ex vivo culture during retroviral transduction without a corresponding increase in SCID repopulating cell (SRC) frequency: dissociation of SRC phenotype and function. *Blood* 95, 102–110. [PubMed: 10607692]
- Dou DR, Calvanese V, Sierra MI, Nguyen AT, Minasian A, Saarikoski P, Sasidharan R, Ramirez CM, Zack JA, Crooks GM, Galic Z, Mikkola HK, 2016. Medial Hoxa genes demarcate haematopoietic stem cell fate during human development. *Nat. Cell. Biol* 18, 595–606. [PubMed: 27183470]
- Doulatov S, Notta F, Laurenti E, Dick JE, 2012. Hematopoiesis: a human perspective. *Cell Stem Cell* 10, 120–136. [PubMed: 22305562]
- Doulatov S, Vo LT, Chou SS, Kim PG, Arora N, Li H, Hadland BK, Bernstein ID, Collins JJ, Zon LI, Daley GQ, 2013. Induction of multipotential hematopoietic progenitors from human

- pluripotent stem cells via respecification of lineage-restricted precursors. *Cell Stem Cell* 13, 459–470. [PubMed: 24094326]
- Frame JM, Fegan KH, Conway SJ, McGrath KE, Palis J, 2016. Definitive hematopoiesis in the yolk sac emerges from Wnt-responsive hemogenic endothelium independently of circulation and arterial identity. *Stem Cells* 34, 431–444. [PubMed: 26418893]
- Fujita A, Uchida N, Haro-Mora JJ, Winkler T, Tisdale J, 2016. beta-globin-expressing definitive erythroid progenitor cells generated from embryonic and induced pluripotent stem cell-derived sacs. *Stem Cells* 34, 1541–1552. [PubMed: 26866725]
- Gering M, Patient R, 2005. Hedgehog signaling is required for adult blood stem cell formation in zebrafish embryos. *Dev. Cell* 8, 389–400. [PubMed: 15737934]
- Goldie LC, Lucitti JL, Dickinson ME, Hirschi KK, 2008. Cell signaling directing the formation and function of hemogenic endothelium during murine embryogenesis. *Blood* 112, 3194–3204. [PubMed: 18684862]
- Gordon-Keylock S, Sobiesiak M, Rybtsov S, Moore K, Medvinsky A, 2013. Mouse extraembryonic arterial vessels harbor precursors capable of maturing into definitive HSCs. *Blood* 122, 2338–2345. [PubMed: 23863896]
- Gori JL, Butler JM, Chan YY, Chandrasekaran D, Poulos MG, Ginsberg M, Nolan DJ, Elemento O, Wood BL, Adair JE, Rafii S, Kiem HP, 2015. Vascular niche promotes hematopoietic multipotent progenitor formation from pluripotent stem cells. *J. Clin. Invest* 125, 1243–1254. [PubMed: 25664855]
- Guibentif C, Rönn R, Böiers C, Lang S, Saxena S, Soneji S, Enver T, Karlsson G, Woods N-B, 2017. Single-cell analysis identifies distinct stages of human endothelial-to-hematopoietic transition. *Cell Rep.* 19, 10–19. [PubMed: 28380349]
- Guzzi N, Ciesla M, Ngoc PCT, Lang S, Arora S, Dimitriou M, Pimkova K, Sommarin MNE, Munita R, Lubas M, Lim Y, Okuyama K, Soneji S, Karlsson G, Hansson J, Jonsson G, Lund AH, Sigvardsson M, Hellstrom-Lindberg E, Hsieh AC, Bellodi C, 2018. Pseudouridylation of tRNA-derived fragments steers translational control in stem cells. *Cell* 173, 1204–1216. [PubMed: 29628141]
- Hadland BK, Varnum-Finney B, Poulos MG, Moon RT, Butler JM, Rafii S, Bernstein ID, 2015. Endothelium and Notch specify and amplify aorta-gonad-mesonephros-derived hematopoietic stem cells. *J. Clin. Invest* 125, 2032–2045. [PubMed: 25866967]
- Han X, Chen H, Huang D, Chen H, Fei L, Cheng C, Huang H, Yuan GC, Guo G, 2018. Mapping human pluripotent stem cell differentiation pathways using high throughput single-cell RNA-sequencing. *Genome Biol.* 19, 47. [PubMed: 29622030]
- He Q, Scott C, Wan C, Flynn RJ, Oster RA, Chen D, Zhang F, Shu Y, Klug CA, 2017. Enhanced hematopoietic stem cell self-renewal-promoting ability of clonal primary mesenchymal stromal/stem cells versus their osteogenic progeny. *Stem Cells* 35, 473–484. [PubMed: 27539014]
- Husa AM, Strobl MR, Strajeriu A, Wieser M, Strehl S, Fortschegger K, 2018. Generation of CD34 fluorescent reporter human induced pluripotent stem cells for monitoring hematopoietic differentiation. *Stem Cells Dev.* 27, 1376–1384. [PubMed: 30009677]
- Ivanovs A, Rybtsov S, Ng ES, Stanley EG, Elefanty AG, Medvinsky A, 2017. Human haematopoietic stem cell development: from the embryo to the dish. *Development* 144, 2323–2337. [PubMed: 28676567]
- Jaffredo T, Gautier R, Eichmann A, Dieterlen-Lievre F, 1998. Intraaortic hemopoietic cells are derived from endothelial cells during ontogeny. *Development* 125, 4575–4583. [PubMed: 9778515]
- Kardel MD, Eaves CJ, 2012. Modeling human hematopoietic cell development from pluripotent stem cells. *Exp. Hematol* 40, 601–611. [PubMed: 22510344]
- Kennedy M, Awong G, Sturgeon CM, Ditadi A, LaMotte-Mohs R, Zuniga-Pflucker JC, Keller G, 2012. T lymphocyte potential marks the emergence of definitive hematopoietic progenitors in human pluripotent stem cell differentiation cultures. *Cell Rep.* 2, 1722–1735. [PubMed: 23219550]
- Kumano K, Chiba S, Kunisato A, Sata M, Saito T, Nakagami-Yamaguchi E, Yamaguchi T, Masuda S, Shimizu K, Takahashi T, Ogawa S, Hamada Y, Hirai H, 2003. Notch1 but not Notch2 is essential for generating hematopoietic stem cells from endothelial cells. *Immunity* 18, 699–711. [PubMed: 12753746]

- Lawson ND, Scheer N, Pham VN, Kim CH, Chitnis AB, Campos-Ortega JA, Weinstein BM, 2001. Notch signaling is required for arterial-venous differentiation during embryonic vascular development. *Development* 128, 3675–3683. [PubMed: 11585794]
- Lawson ND, Vogel AM, Weinstein BM, 2002. sonic hedgehog and vascular endothelial growth factor act upstream of the Notch pathway during arterial endothelial differentiation. *Dev. Cell* 3, 127–136. [PubMed: 12110173]
- Mazzoni EO, Mahony S, Peljto M, Patel T, Thornton SR, McCuine S, Reeder C, Boyer LA, Young RA, Gifford DK, Wichterle H, 2013. Saltatory remodeling of Hox chromatin in response to rostrocaudal patterning signals. *Nat. Neurosci* 16, 1191–1198. [PubMed: 23955559]
- McQuade A, Coburn M, Tu CH, Hasselmann J, Davtyan H, Blurton-Jones M, 2018. Development and validation of a simplified method to generate human microglia from pluripotent stem cells. *Mol. Neurodegener* 13, 67. [PubMed: 30577865]
- Montavon T, Soshnikova N, 2014. Hox gene regulation and timing in embryogenesis. *Semin. Cell Dev. Biol* 34, 76–84. [PubMed: 24930771]
- Ng ES, Azzola L, Bruveris FF, Calvanese V, Phipson B, Vlahos K, Hirst C, Jokubaitis VJ, Yu QC, Maksimovic J, Liebscher S, Januar V, Zhang Z, Williams B, Conscience A, Durnall J, Jackson S, Costa M, Elliott D, Haylock DN, Nilsson SK, Saffery R, Schenke-Layland K, Oshlack A, Mikkola HK, Stanley EG, Elefanty AG, 2016. Differentiation of human embryonic stem cells to HOXA(+) hemogenic vasculature that resembles the aorta-gonad-mesonephros. *Nat. Biotechnol* 34, 1168–1179. [PubMed: 27748754]
- Notta F, Doulatov S, Laurenti E, Poepl A, Jurisica I, Dick JE, 2011. Isolation of single human hematopoietic stem cells capable of long-term multilineage engraftment. *Science* 333, 218–221. [PubMed: 21737740]
- Park MA, Kumar A, Jung HS, Uenishi G, Moskvina OV, Thomson JA, Slukvin II, 2018. Activation of the arterial program drives development of definitive hemogenic endothelium with lymphoid potential. *Cell Rep.* 23, 2467–2481. [PubMed: 29791856]
- Perucca S, Di Palma, A, Piccaluga PP, Gemelli C, Zoratti E, Bassi G, Giacomuzzi E, Lojcono A, Borsani G, Tagliafico E, Scupoli MT, Bernardi S, Zanaglio C, Cattina F, Cancelli V, Malagola M, Krampera M, Marini M, Almicci C, Ferrari S, Russo D, 2017. Mesenchymal stromal cells (MSCs) induce ex vivo proliferation and erythroid commitment of cord blood haematopoietic stem cells (CB-CD34+ cells). *PLoS ONE* 12, e0172430. [PubMed: 28231331]
- Robert-Moreno A, Espinosa L, de la Pompa JL, Bigas A, 2005. RBPj κ -dependent Notch function regulates Gata2 and is essential for the formation of intra-embryonic hematopoietic cells. *Development* 132, 1117–1126. [PubMed: 15689374]
- Robert-Moreno A, Guiu J, Ruiz-Herguido C, Lopez ME, Ingles-Esteve J, Riera L, Tipping A, Enver T, Dzierzak E, Gridley T, Espinosa L, Bigas A, 2008. Impaired embryonic haematopoiesis yet normal arterial development in the absence of the Notch ligand Jagged1. *EMBO J.* 27, 1886–1895. [PubMed: 18528438]
- Rybtsov SA, Lagarkova MA, 2019. Development of hematopoietic stem cells in the early mammalian embryo. *Biochemistry (Mosc)* 84, 190–204. [PubMed: 31221058]
- Slukvin II, Uenishi GI, 2019. Arterial identity of hemogenic endothelium: a key to unlock definitive hematopoietic commitment in human pluripotent stem cell cultures. *Exp. Hematol* 71, 3–12. [PubMed: 30500414]
- Snyder KM, Hullsiek R, Mishra HK, Mendez DC, Li Y, Rogich A, Kaufman DS, Wu J, Walcheck B, 2018. Expression of a recombinant high affinity IgG Fc receptor by engineered NK cells as a docking platform for therapeutic mAbs to target cancer cells. *Front. Immunol* 9, 2873. [PubMed: 30574146]
- Sturgeon CM, Chicha L, Ditadi A, Zhou Q, McGrath KE, Palis J, Hammond SM, Wang S, Olson EN, Keller G, 2012. Primitive erythropoiesis is regulated by miR-126 via nonhematopoietic Vcam-1+ cells. *Dev. Cell* 23, 45–57. [PubMed: 22749417]
- Sturgeon CM, Ditadi A, Awong G, Kennedy M, Keller G, 2014. Wnt signaling controls the specification of definitive and primitive hematopoiesis from human pluripotent stem cells. *Nat. Biotechnol* 32, 554–561. [PubMed: 24837661]

- Sugimura R, Jha DK, Han A, Soria-Valles C, da Rocha EL, Lu YF, Goettel JA, Serrao E, Rowe RG, Malleshaiah M, Wong I, Sousa P, Zhu TN, Ditadi A, Keller G, Engelman AN, Snapper SB, Doulatov S, Daley GQ, 2017. Haematopoietic stem and progenitor cells from human pluripotent stem cells. *Nature* 545, 432–438. [PubMed: 28514439]
- Uchida N, Haro-Mora JJ, Demirci S, Fujita A, Raines L, Hsieh MM, Tisdale JF, 2018. High-level embryonic globin production with efficient erythroid differentiation from a K562 erythroleukemia cell line. *Exp. Hematol* 62, 7–16 e11. [PubMed: 29524566]
- Uchida N, Haro-Mora JJ, Fujita A, Lee DY, Winkler T, Hsieh MM, Tisdale JF, 2017. Efficient generation of beta-globin-expressing erythroid cells using stromal cell-derived induced pluripotent stem cells from patients with sickle cell disease. *Stem Cells* 35, 586–596. [PubMed: 27739611]
- Uenishi GI, Jung HS, Kumar A, Park MA, Hadland BK, McLeod E, Raymond M, Moskvina O, Zimmerman CE, Theisen DJ, Swanson S, O.J.T., Zon LI, Thomson JA, Bernstein ID, 2018. NOTCH signaling specifies arterial-type definitive hemogenic endothelium from human pluripotent stem cells. *Nat. Commun* 9, 1828. [PubMed: 29739946]
- Vo LT, Daley GQ, 2015. De novo generation of HSCs from somatic and pluripotent stem cell sources. *Blood* 125, 2641–2648. [PubMed: 25762177]
- Walasek MA, van Os R, de Haan G, 2012. Hematopoietic stem cell expansion: challenges and opportunities. *Ann. N. Y. Acad. Sci* 1266, 138–150. [PubMed: 22901265]
- Yoder MC, 2014. Inducing definitive hematopoiesis in a dish. *Nat. Biotechnol* 32,539–541. [PubMed: 24911496]
- Yzaguirre AD, Speck NA, 2016. Insights into blood cell formation from hemogenic endothelium in lesser-known anatomic sites. *Dev. Dyn* 245, 1011–1028. [PubMed: 27389484]
- Zovein AC, Hofmann JJ, Lynch M, French WJ, Turlo KA, Yang Y, Becker MS, Zanetta L, Dejana E, Gasson JC, Tallquist MD, Iruela-Arispe ML, 2008. Fate tracing reveals the endothelial origin of hematopoietic stem cells. *Cell Stem Cell* 3, 625–636. [PubMed: 19041779]

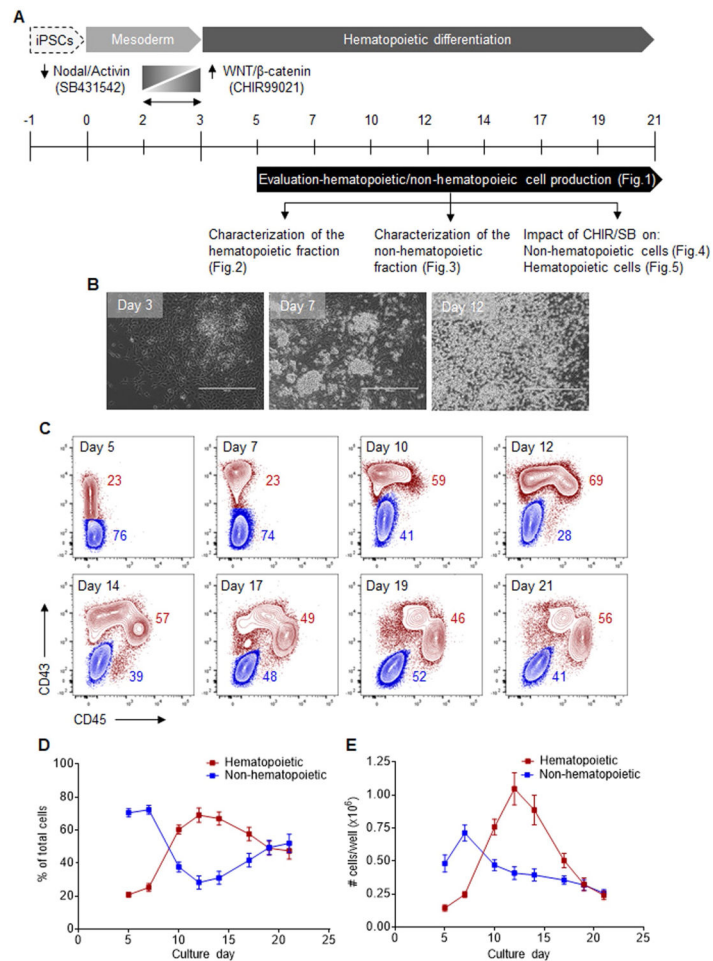


Fig. 1. Robust production of an adherent monolayer and supernatant hematopoietic cells during differentiation of human iPSCs. (A) Schematic of the experimental design for hematopoietic differentiation of human iPSCs, including mesodermal (day 0 to 3) and hematopoietic (day 3 to 21) differentiation steps. Long vertical bars represent full medium changes or initiation/end of culture, and short vertical bars indicate half medium changes. All cells were harvested for analyses at the indicated intervals from day 5 to 21 of culture. In select experiments, WNT/β-catenin agonist CHIR99021 (CHIR) and activin/nodal/TGFβ antagonist SB431542 (SB) were added on day 2 for 24–36 h. (B) Representative phase-contrast microscopy images taken at various days of differentiation: day 3, adherent monolayer formation with the emergence of mesodermal colonies; day 7, hematopoietic clusters arising from the adherent monolayer; day 12, suspension hematopoietic cells. Scale bar = 400 μm. (C) Representative flow cytometry overlay plots for CD43 and CD45 expression, depicting CD43⁻CD45⁻ non-hematopoietic cells (blue) and CD43⁺CD45^{+/-} hematopoietic cells (red) at various days of differentiation. The complete gating strategy is shown in Fig. S1A. (D) Percentages of hematopoietic and non-hematopoietic cells at various days of differentiation ($n = 6$). (E) Absolute numbers of hematopoietic and non-hematopoietic cells arising from 20 to 35 iPSC clusters (one well of a 12-well plate) at various days of differentiation ($n = 6$). In panels (D) and (E), results are displayed as mean

± SEM. (For interpretation of the references to colour in this figure legend, the reader is referred to the web version of this article.)

Author Manuscript

Author Manuscript

Author Manuscript

Author Manuscript

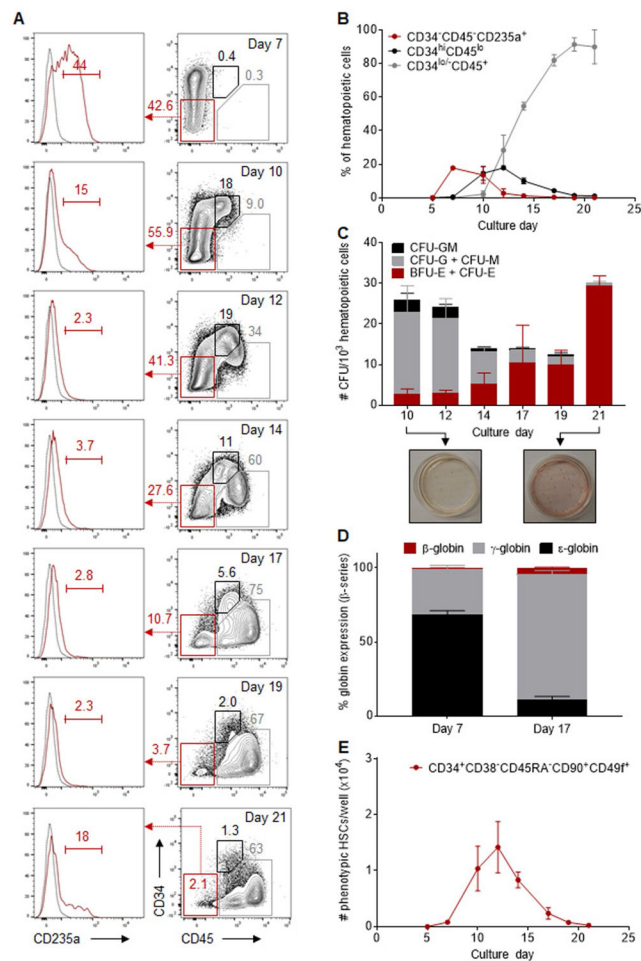


Fig. 2. Successive emergence of primitive and definitive hematopoietic populations during differentiation of human iPSCs. (A) Representative flow cytometry plots for CD34, CD45 and CD235a expression in gated CD43⁺CD45^{+/-} hematopoietic cells at various days of differentiation. Gates shown include: CD34⁻CD45⁻CD235a⁺ primitive erythroid progenitors (red), CD34^{hi}CD45^{lo} multilineage HSPCs (black), and CD34^{lo/-}CD45⁺ hematopoietic progenitors (gray). The complete gating strategy is shown in Fig. S1B. (B) Percentage of hematopoietic populations with immunophenotypes classified above within the CD43⁺CD45^{+/-} hematopoietic fraction at various days of differentiation ($n = 3$). (C) CFU counts per 1000 sorted hematopoietic cells at various days of differentiation ($n = 6$). Insets at the bottom are representative CFU plates demonstrating multilineage HSPCs at day 10 and almost exclusive production of erythroid progenitors at day 21 of culture. (D) Percentage of β -globin series expression in erythroid cells differentiated from day 7 and 17 supernatant cells ($n = 3$), measured by RP-HPLC. (E) Absolute numbers of CD43⁺CD45⁺ hematopoietic cells with a CD34⁺CD38⁻CD45RA⁻CD90⁺CD49f⁺ immunophenotype arising from 20 to 35 iPSC clusters (one well of a 12-well plate) at various days of differentiation ($n = 3$). In panels (B) to (E), results are displayed as mean \pm SEM. (For interpretation of the references to colour in this figure legend, the reader is referred to the web version of this article.)

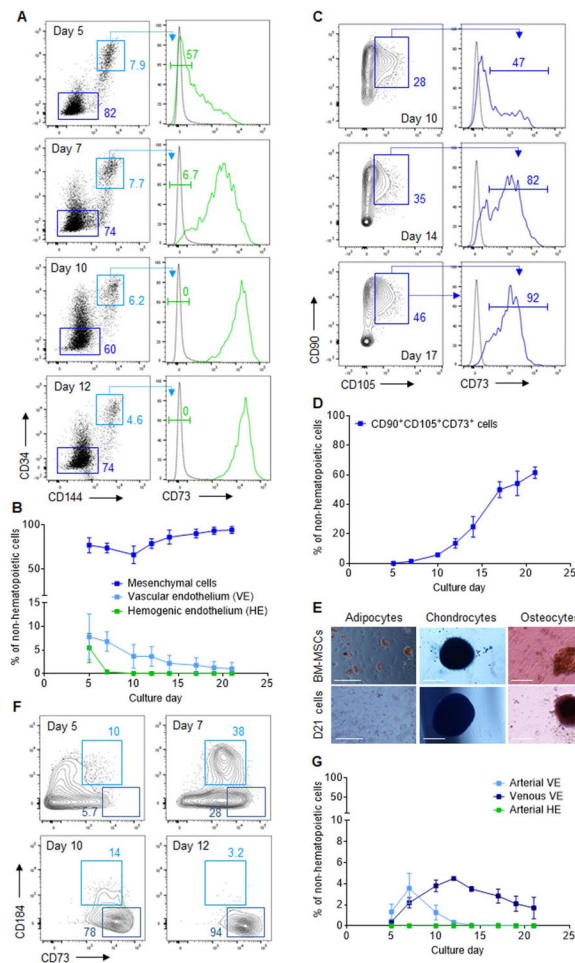


Fig. 3. Abundant mesenchymal cells and limited arterial endothelium formation during human iPSC differentiation. (A) Representative flow cytometry plots for CD34, CD144 (VE-cadherin) and CD73 expression in gated CD43⁻CD45⁻ non-hematopoietic cells at various days of differentiation. Gates shown include: CD144⁻CD34⁻ mesenchymal cells (dark blue), CD144⁺CD34^{hi} vascular endothelium (VE, light blue), and CD144⁺CD34^{hi}CD73⁻ hemogenic endothelium (HE, green). The complete gating strategy is shown in Fig. S1C. (B) Percentage of cells with a mesenchymal, VE or HE immunophenotype within the non-hematopoietic fraction at various days of differentiation ($n = 3$). (C) Representative flow cytometry plots of CD90, CD105 and CD73 expression in gated CD144⁻CD34⁻ mesenchymal cells at various days of differentiation. The complete gating strategy is shown in Fig. S1 D. (D) Percentage of cells with a CD90⁺CD105⁺CD73⁺ mesenchymal stromal cell (MSC) immunophenotype within the CD43⁻CD45⁻ non-hematopoietic fraction at various days of differentiation ($n = 3$). (E) Representative images depicting adipocyte (Oil Red O stain), chondrocytes (Alcian Blue stain), and osteocytes (Alizarin Red stain) after culture of control BM-derived MSCs (top panels) or day 21 sorted CD43⁻CD45⁻ cells (bottom panels) under conditions promoting differentiation of each cell type ($n = 2$). Scale bar = 100 μ m (adipocytes panels) or 200 μ m (chondrocytes and osteocytes panels). (F) Representative flow cytometry plots for CD184 and CD73 expression in

gated CD144⁺CD34^{hi} VE cells. Gates shown include: CD73^{mid}CD184⁺ arterial VE (light blue), and CD73^{hi}CD184⁻ venous VE (dark blue). The complete gating strategy is shown in Fig. S1E. (G) Percentage of cells with an arterial VE, venous VE or arterial HE immunophenotype within the non-hematopoietic fraction at various days of differentiation ($n = 3$). In panels (B), (D), and (G), results are displayed as mean \pm SEM. (For interpretation of the references to colour in this figure legend, the reader is referred to the web version of this article.)

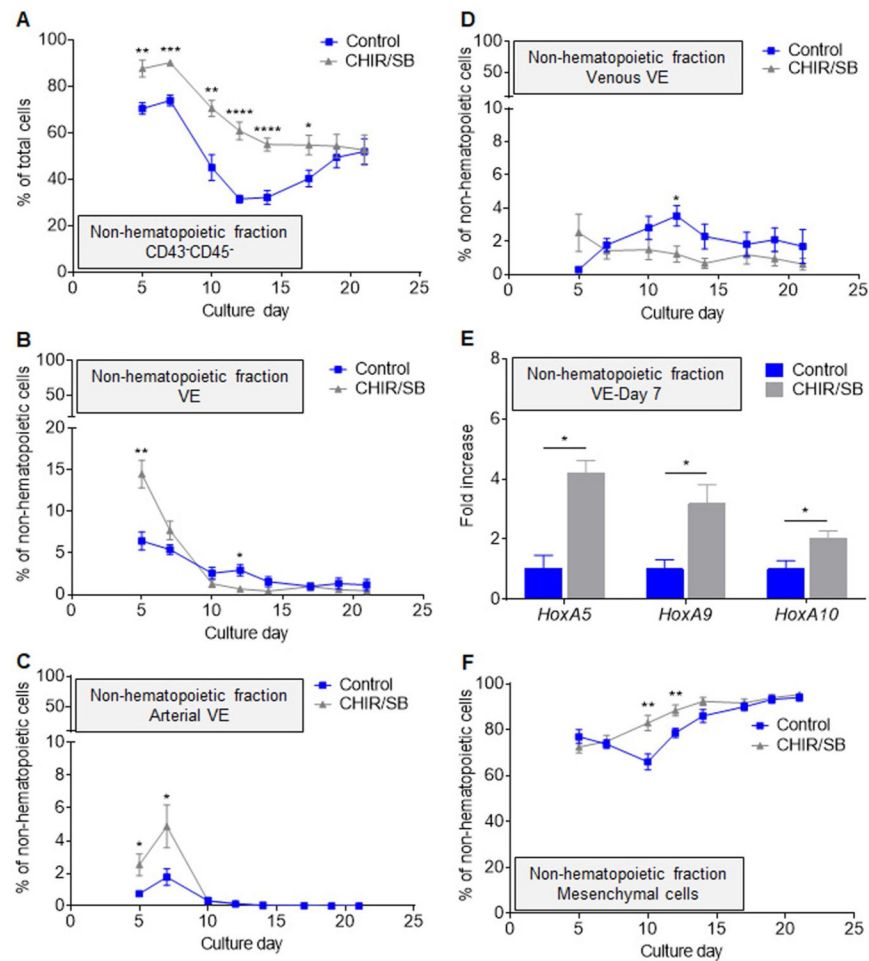


Fig. 4. CHIR/SB molecules increase arterial endothelium formation during the early phase of human iPSC differentiation. (A) Percentage of CD43⁻CD45⁻ non-hematopoietic cells in control and CHIR/SB-supplemented cultures at various days of differentiation ($n = 8$). (B) Percentage of CD144⁺CD34^{hi} VE cells within the non-hematopoietic fraction of control and CHIR/SB-supplemented cultures at various days of differentiation ($n = 7$). (C) Percentage of CD73^{mid}CD184⁺ arterial VE cells within the non-hematopoietic fraction of control and CHIR/SB-supplemented cultures at various days of differentiation ($n = 7$). (D) Percentage of CD73^{hi}CD184⁻ venous VE cells within the non-hematopoietic fraction of control and CHIR/SB-supplemented cultures at various days of differentiation ($n = 5$). (E) Fold increase in HOXA gene expression measured by real-time qPCR in CD144⁺CD34^{hi} VE cells sorted from CHIR/SB-supplemented cultures at day 7 of differentiation relative to the same population sorted from control cultures ($n = 3$). (F) Percentage of CD144⁻CD34⁻ mesenchymal cells within the non-hematopoietic fraction of control and CHIR/SB-supplemented cultures at various days of differentiation ($n = 5$). Results are displayed as mean \pm SEM; * $P < 0.05$, ** $P < 0.01$, *** $P < 0.001$, **** $P < 0.0001$, by two-way unpaired Student's t-tests comparing percentages of cells (A-D and F), or day 7 untransformed CT values (E) in control vs CHIR/SB groups at each culture day.

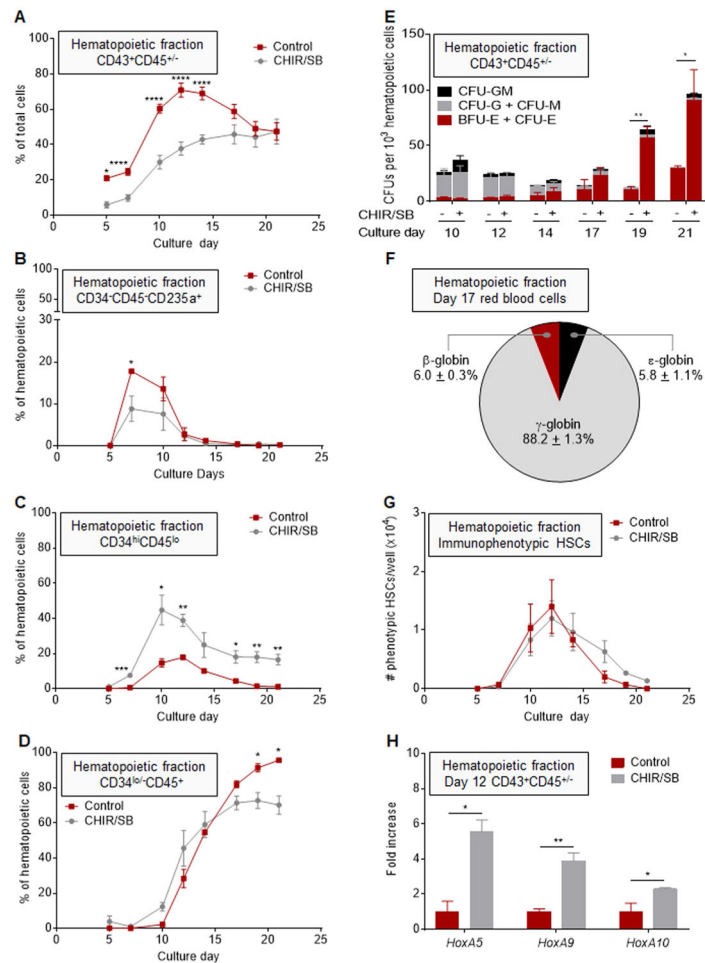


Fig. 5. CHIR/SB molecules suppress primitive hematopoiesis and promote definitive HSPC formation during human iPSC differentiation. (A) Percentage of CD43⁺CD45^{+/-} hematopoietic cells in control and CHIR/SB-supplemented cultures at various days of differentiation ($n = 8$). (B) Percentage of CD34⁻CD45⁻CD235a⁺ primitive erythroid progenitor cells within the hematopoietic fraction of control and CHIR/SB-supplemented cultures at various days of differentiation ($n = 5$). (C) Percentage of CD34^{hi}CD45^{lo} multilineage HSPCs within the hematopoietic fraction of control and CHIR/SB-supplemented cultures at various days of differentiation ($n = 5$). (D) Percentage of CD34^{lo/-}CD45⁺ hematopoietic progenitors within the hematopoietic fraction of control and CHIR/SB-supplemented cultures at various days of differentiation ($n = 5$). (E) CFU counts per 1×10^3 CD43⁺CD45^{+/-} hematopoietic cells sorted from control and CHIR/SB-supplemented cultures at various days of differentiation ($n = 8$). (F) Percentage of β -globin series expression measured by RP-HPLC in erythroid cells differentiated from day 17 hematopoietic cells of CHIR/SB-supplemented cultures ($n = 2$). (G) Absolute numbers of CD34⁺CD38⁻CD45RA⁻CD90⁺CD49f⁺ cells within the CD43⁺CD45⁺ hematopoietic fraction arising from 20 to 35 iPSC clusters (one well of a 12-well plate) in control and CHIR/SB-supplemented cultures at various days of differentiation ($n = 3$). (H) Fold increase in HOXA gene expression measured by real-time qPCR in CD43⁺CD45^{+/-} hematopoietic

cells sorted from CHIR/SB-supplemented cultures at D12 of differentiation relative to the same population sorted from control cultures ($n = 3$). Results are displayed as mean \pm SEM; * $P < 0.05$, ** $P < 0.01$, *** $P < 0.001$, **** $P < 0.0001$, by two-way unpaired Student's t-tests comparing percentages (A-D), CFU counts (E), cell numbers (G), or day 7 untransformed CT values (H) in control vs CHIR/SB groups at each culture day.

Author Manuscript

Author Manuscript

Author Manuscript

Author Manuscript

KEY RESOURCES TABLE

Reagent or resource	Source	Identifier
Antibodies		
CD34 PE-Cy7 Mouse anti-human	BD Pharmingen	560710
CD34 PE Mouse anti-human	BD Pharmingen	555822
CD38 APC Mouse anti-human	BD Pharmingen	555462
CD43 BV711 Mouse anti-human	BD OptiBuild	743614
CD43 FITC Mouse anti-human	BD Pharmingen	555475
CD45 V450 Mouse anti-human	BD Horizon	560367
CD45RA APC—H7 Mouse anti-human	BD Pharmingen	560674
CD49f PE-Cy5 Rat anti-human	BD Pharmingen	551129
CD73 PE Mouse anti-human	BD Pharmingen	550257
CD73 FITC Mouse anti-human	BD Pharmingen	561254
CD90 PE-Cy7 Mouse anti-human	BD Pharmingen	561558
CD105 AF647 Mouse anti-human	BD Pharmingen	561439
CD144 BV605 Mouse anti-human	BD OptiBuild	743705
CD184 PE-CF594 Mouse anti-human	BD Horizon	562389
CD235a FITC Mouse anti-human	Biologend	349104
Bacterial and Virus Strains		
Biological Samples		
Chemicals, Peptides, and Recombinant	Proteins	
ROCK Inhibitor	Sigma	Y0503
CHIR99021	Sigma	SML1046
SB431542	Sigma	S4317
Erythropoietin (EPOGEN®)	Amgen	NDC 55513-126-10
Interleukin-3 (IL3)	R&D Systems	203-IL
Stem Cell Factor (SCF)	R&D Systems	255-SC
Estradiol	Pfizer	NDC 0009-0271-01
Dexamethasone	VEtone	NDC 13985-533-03
Knockout Replacement Serum	ThermoFisher	10828028
Transferrin	Sigma Aldrich	T4132–1 G
Bovine Serum Albumin	Roche	03116956001
Insulin	Lilly	Humulin R HI210
Critical Commercial Assays		
RNEasy Micro Kit	Qiagen	74004
Taqman RNA-to-Ct 1-Step Kit	Applied Biosystems	4392653
MethoCult H4435 Enriched Human CFU Assay	STEMCELL Technologies, Inc.	04445
Adipocyte Differentiation Assay	ThermoFisher	A1007001
Chondrocyte Differentiation Assay	ThermoFisher	A1007101
Osteocyte Differentiation Assay	ThermoFisher	A1007201
Deposited Data		
Experimental Models: Cell Lines		

Reagent or resource	Source	Identifier
MCND-TENS2 Line	This Paper	RTIBDi001-A
OP9	ATCC	CRL-2749
Experimental Models: Organisms/Strains		
Female NSG Mice	Jackson Laboratory	05557
Oligonucleotides		
GAPDH – VIC	Life Technologies	Hs03929097_g1
HoxA5 – FAM	Life Technologies	Hs00430330_m1
HoxA9 – FAM	Life Technologies	Hs00365956_m1
HoxA10 – FAM Recombinant DNA	Life Technologies	Hs00172012_m1
Software and Algorithms		
FlowJo 10.5.3	FlowJo, LLC	N/A
GraphPad Prism 7.02	GraphPad Software, Inc.	
Other		
Matrigel	Corning	354230
Essential 8 Medium	ThermoFisher	A1517001
STEMdiff™ Hematopoietic Kit	STEMCELL Technologies, Inc.	05310
7-AAD	Thermofisher	00-6993-50
Accutase	STEMCELL Technologies, Inc.	07920